JACS
JOURNAL OF THE AMERICAN CHEMICAL SOCIETY
Article
pubs.acs.org/JACS

Causation in a Cascade: The Origins of Selectivities in Intramolecular Nitrone Cycloadditions

Elizabeth H. Krenske,*[,†,‡] Sesil Agopcan,[§] Viktorya Aviyente,[§] K. N. Houk,*[,∥] Brian A. Johnson,[†] and Andrew B. Holmes*[,†,⊥]

[†]School of Chemistry, University of Melbourne, VIC 3010, Australia
[‡]Australian Research Council Centre of Excellence for Free Radical Chemistry and Biotechnology
[§]Chemistry Department, Bogazici University, 34342 Bebek, Istanbul, Turkey
[∥]Department of Chemistry and Biochemistry, University of California, Los Angeles, California 90095, United States
[⊥]CSIRO Materials Science and Engineering, Bag 10, Clayton South, VIC 3169, Australia

Supporting Information

ABSTRACT: The factors controlling chemo-, regio-, and stereoselectivity in a cascade of reactions starting from a bis(cyanoalkenyl)oxime and proceeding via nitrone cycloadditions have been unraveled through a series of density functional theory calculations with several different functionals. Both kinetic and thermodynamic control of the reaction cascade are important, depending upon the conditions. Kinetic control was analyzed by the distortion/interaction model and found to be dictated by differences in distortions of the cycloaddends in the transition states. A new mechanism competing with that originally proposed in the application of these reactions to the histrionicotoxin synthesis was discovered in these studies.

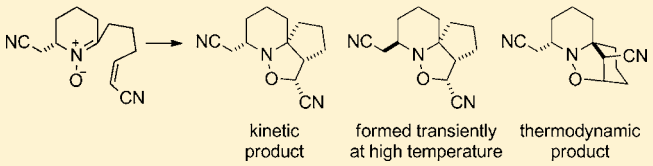

INTRODUCTION

Intramolecular 1,3-dipolar cycloadditions are an important tool for the assembly of complex molecular architectures.[1] Holmes[2] and Stockman[3] used an intramolecular 1,3-dipolar cycloaddition between a nitrone and a cyano-substituted alkene as a key step in the synthesis of histrionicotoxin alkaloids (Scheme 1). The crucial 6,6,5-tricyclic intermediate **6** is derived from an intramolecular 1,3-dipolar cycloaddition of *C*-(cyanoalkenyl)-nitrone **3**. The nitrone is generated from the symmetrical ketone **1** via oxime **2** (NH_2OH·HCl/NaOAc, methanol, 50 °C) and undergoes intramolecular 1,3-dipolar cycloaddition spontaneously under these conditions. However, there are in total four regio- and stereochemically distinct modes of cycloaddition,[4] and the major product at 50 °C is not **6** but the 6,5,5-tricyclic species **4**. Cycloadduct **4** is converted to **6** (the thermodynamically favored cycloadduct) by thermal equilibration (e.g., 180 °C, chlorobenzene).[5]

During experimental efforts to optimize the yield of the desired 6,6,5 cycloadduct **6**, we uncovered two intriguing phenomena:

(1) A second 6,5,5-tricyclic species, **5** (Scheme 1), is formed transiently during the thermal isomerization of **4** to **6**.[2d]
(2) An enantiomerically pure sample of (+)-**6**, when heated at 185 °C in chlorobenzene for 16 h, was found to undergo racemization.[2d]

These observations were proposed to arise through the series of interconversions shown in Scheme 2.[2d] In this scheme, we use primes to denote enantiomeric species whose optical rotations are not known. The racemization of (+)-**6** commences at the lower left with a retro-1,3-dipolar cycloaddition to form **3**. Cycloaddition in the opposite regio- and stereochemical sense then gives **5**. Opening of the piperidine ring of **5** leads to bicyclic species **8**, which recyclizes from the opposite face to give **4**. Retro-1,3-dipolar cycloaddition followed by recycloaddition in the opposite regio- and stereochemical sense gives (−)-**6**.

Here we report a computational investigation of the tandem oxime cyclization/1,3-dipolar cycloaddition route to the histrionicotoxin precursor **6**. The origins of thermodynamic and kinetic control in the intramolecular 1,3-dipolar cycloaddition of **3** and the mechanism of the thermal racemization of (+)-**6** were explored with density functional theory computations. The calculations support the proposed racemization mechanism (Scheme 2) but also predict a second pathway that involves opening of the piperidine ring of (+)-**6** through an elimination reaction.

COMPUTATIONAL METHODS

Geometries of reactants, transition states, and products were optimized at the B3LYP/6-31+G(d) level[6] in Gaussian 03.[7] Conformational searching was performed at the PM3 level in Spartan 08[8] and at the B3LYP/6-31+G(d) level. Frequency calculations at the B3LYP/6-31+G(d) level were used to determine the nature of minima and transition states, and intrinsic reaction coordinate calculations[9]

Received: January 1, 2012
Published: July 12, 2012

   dx.doi.org/10.1021/ja300002k | J. Am. Chem. Soc. 2012, 134, 12010−12015

Scheme 1. Holmes–Stockman Intramolecular Nitrone 1,3-Dipolar Cycloaddition Route to Histrionicotoxin[2,3]

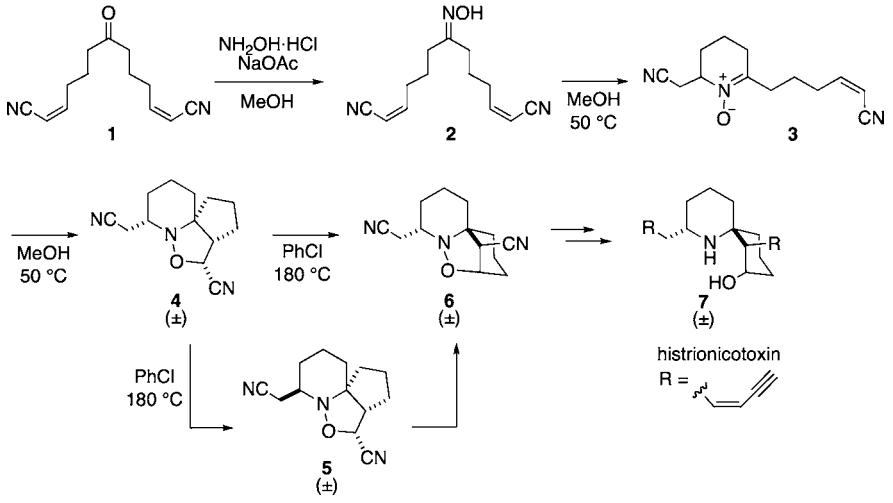

Scheme 2. Mechanism Previously Proposed for the Racemization of (+)-6[2d]

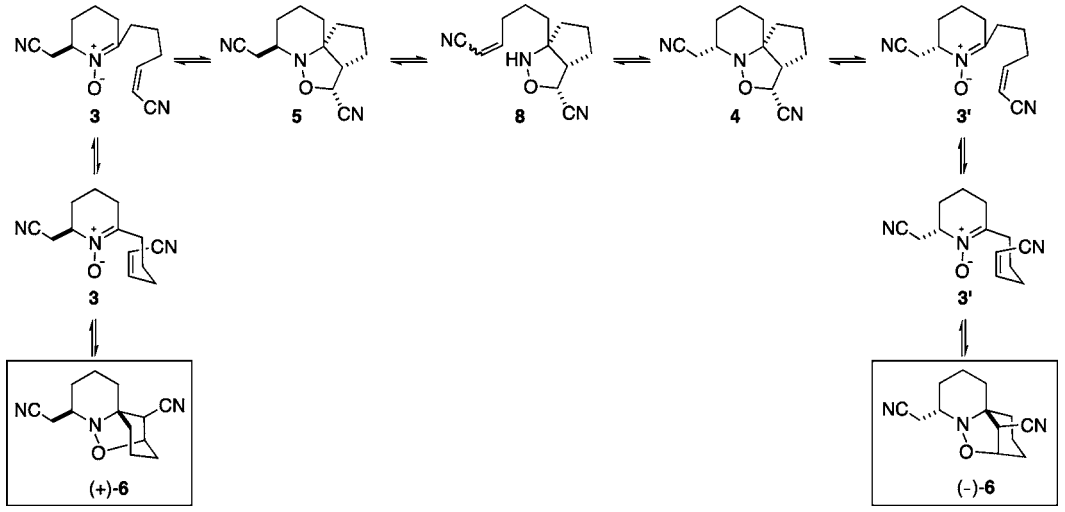

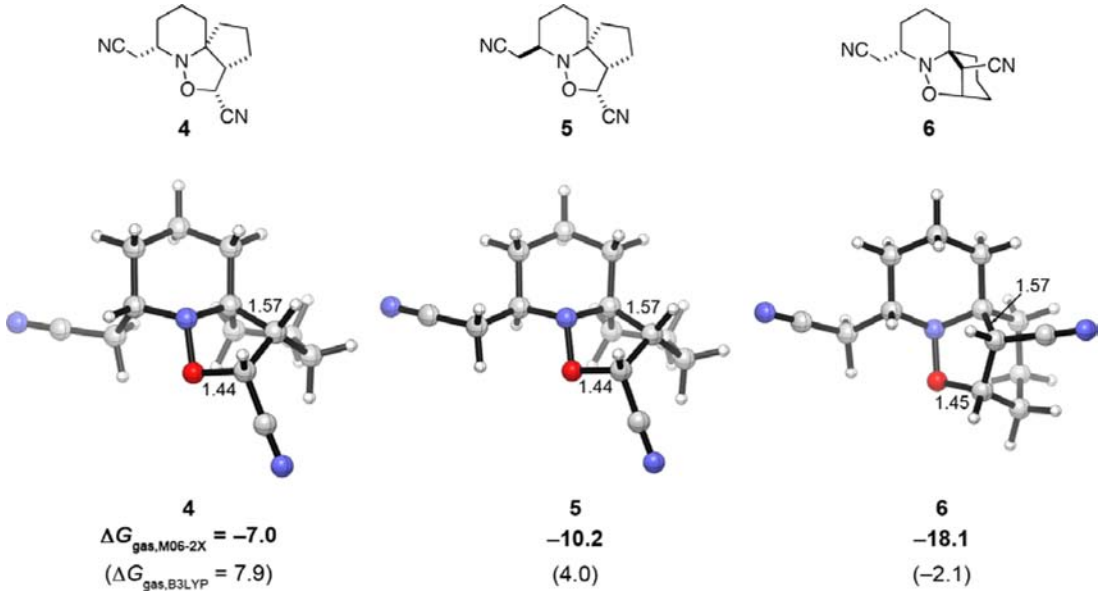

Figure 1. Structures of the tricyclic products **4**, **5**, and **6** calculated at the B3LYP/6-31+G(d) level. M06-2X Gibbs free energies (kcal/mol) relative to nitrone **3** are shown in bold, with B3LYP values in parentheses. Bond lengths are in Å.

dx.doi.org/10.1021/ja300002k | J. Am. Chem. Soc. 2012, 134, 12010–12015

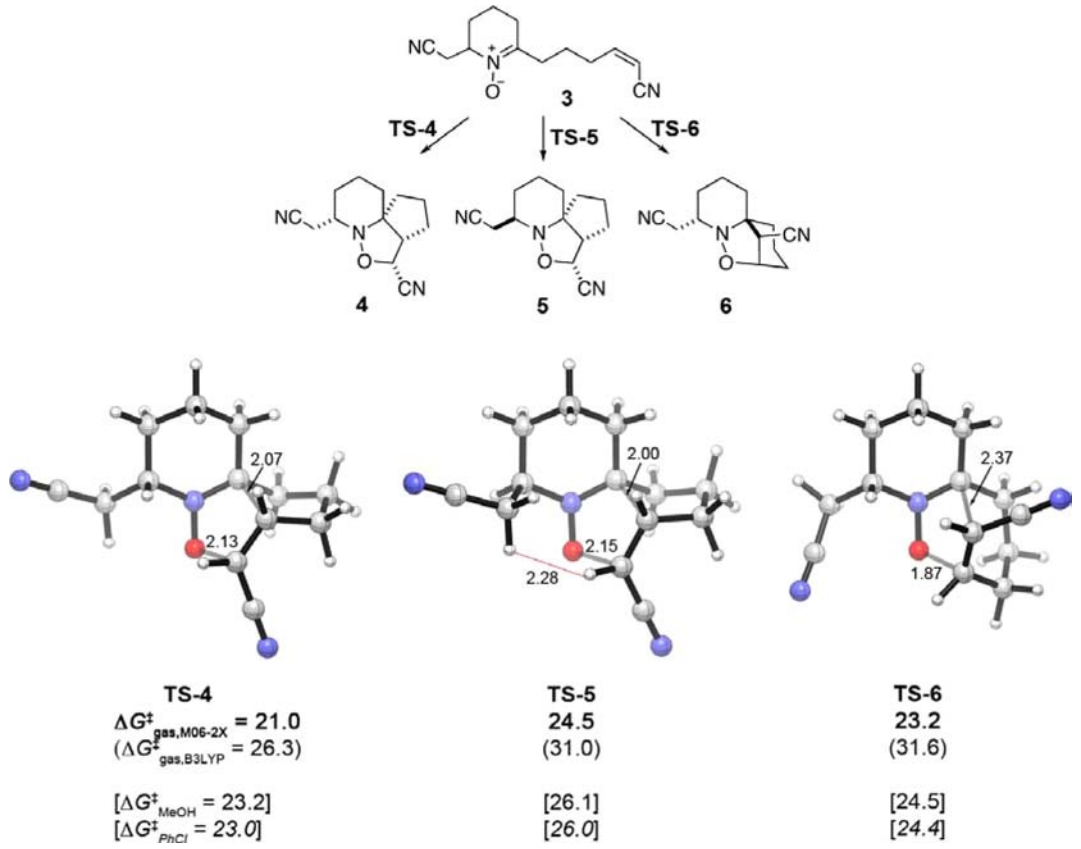

Figure 2. Transition structures for intramolecular 1,3-dipolar cycloadditions of nitrone **3** leading to the tricyclic species **4**, **5**, and **6** calculated at the B3LYP/6-31+G(d) level. Below each structure are listed the Gibbs free energies of activation in the gas phase calculated by M06-2X (bold) and B3LYP (in parentheses), along with solution values in methanol (in brackets) and chlorobenzene (italic, in brackets). Activation energies (kcal/mol) are calculated with respect to **3**. Bond lengths are in Å.

were used to characterize transition states where appropriate. Zero-point energies and thermal corrections were obtained from the B3LYP frequency analyses and are unscaled. Single-point energies were subsequently calculated at the M06-2X/6-311+G(d,p) level[10] in Gaussian 09.[11] M06-2X free energies were computed from the M06-2X electronic energies by addition of the B3LYP zero-point and thermochemical corrections. The geometries of **4**–**6** and **TS-4**–**TS-6** were also optimized at the M06-2X/6-31+G(d) level. Optimization with M06-2X led to minor differences in the geometries, reaction energies, and activation energies; these are described in the Supporting Information. The effects of solvent were studied by means of single-point calculations with the CPCM method[12] (UAKS radii) at the M06-2X/6-31+G(d) level in methanol or chlorobenzene (Gaussian 09). Free energies are quoted at 298.15 K and 1 mol/L. Computed molecular structures were drawn with the CYLview program.[13]

RESULTS AND DISCUSSION

Thermodynamic Control. We first performed calculations to examine the relative thermodynamic stabilities of the cycloadducts **4**–**6**. Geometries of the cycloadducts were optimized at the B3LYP/6-31+G(d) level, and single-point energies were then calculated at the M06-2X/6-311+G(d,p) level. The optimized geometries of **4**–**6** are shown in Figure 1, along with their free energies relative to nitrone **3** (M06-2X in bold, B3LYP in parentheses).

Consistent with experiment, both M06-2X and B3LYP predict the 6,6,5-tricyclic species **6** to be the thermodynamic product. This cycloadduct lies 7.9 kcal/mol below **5** and 11.1 kcal/mol below **4** at the M06-2X level. At the B3LYP level, **6** lies 6.1 kcal/mol below **5** and 10.0 kcal/mol below **4**. The tricyclic species **4**–**6** have previously been studied at the B3LYP/6-31G(d) level, which gave relative energies (ΔE) of 5.8, 4.5, and 0 kcal/mol, respectively.[2d] The B3LYP data in Figure 1 underestimate the thermodynamic stabilities of the cycloadducts, predicting only **6** to be lower in energy than the starting nitrone. In contrast, M06-2X predicts all three cycloadducts to be lower in energy than **3**. Recent benchmarking studies have shown that B3LYP in conjunction with the 6-31+G(d) basis set underestimates the exothermicity of the parent 1,3-dipolar cycloaddition between methylene nitrone and ethylene by 5 kcal/mol.[14] Substantial underestimation of reaction enthalpies by B3LYP has also been reported for Diels–Alder reactions of CN-substituted alkenes.[15]

Within the 6,5,5 series, **5** has the CH_2CN group in an equatorial position and is consequently favored by 3–4 kcal/mol over the axial isomer **4**. The greater stability of the 6,6,5-tricyclic adduct **6** relative to either **4** or **5** is due both to a greater inherent stability of the 6,6,5-tricyclic core and to additional influences of the appended substituents. The 6,6,5 core is 4 kcal/mol more stable than the 6,5,5 core when the CN and CH_2CN groups are replaced by hydrogen atoms (see the Supporting Information).

Kinetic Control. Under conditions of kinetic control (methanol, 50 °C), the intramolecular cycloaddition of **3** furnishes the least stable cycloadduct, **4**, in greatest amount. To explain this, transition states were calculated for the formation of **4**–**6** from the common nitrone precursor **3**. Their structures are shown in Figure 2. Gas-phase activation energies (M06-2X and B3LYP) are shown below each structure, together with

solution-phase values in methanol and chlorobenzene obtained from CPCM calculations.

Both M06-2X and B3LYP correctly predict **4** to be the kinetic product. The M06-2X activation energies lie within the range 21.0−24.5 kcal/mol and are more consistent with the experimental conditions than are the B3LYP values, which are 5−8 kcal/mol higher. The activation energy for the formation of **4** (**TS-4**, $\Delta G^{\ddagger}$ = 21.0 kcal/mol) is 2.2 kcal/mol smaller than that for the formation of **6** and 3.5 kcal/mol smaller than for **5**. These values correspond to a **4**:**5**:**6** ratio of 96:0:3 under kinetic control at 50 °C.

Within the 6,5,5 series, the kinetic preference for **4** over **5** arises from steric effects. Axial−equatorial energy differences in the transition states are not large, because the nitrone is still relatively flat. The pseudoequatorial **TS-5** is disfavored by 3−5 kcal/mol relative to the pseudoaxial **TS-4** because of steric crowding between the CH_2CN group and the approaching alkene. A close H−H distance of 2.28 Å is present in **TS-5** (see the red line in Figure 2), which is absent in **TS-4**.

To explain why **4** is also kinetically favored over **6**, we evaluated the strain energies present in various fragments of the transition states **TS-4** and **TS-6**.[16] Separate calculations were performed on the nitrone ring, the tether connecting the nitrone to the alkene, and the five-membered bond-forming array. Most of the energy difference was found to arise from poor alignment of the reacting groups in the five-membered bond-forming array. In Figure 3 are shown the bond-forming

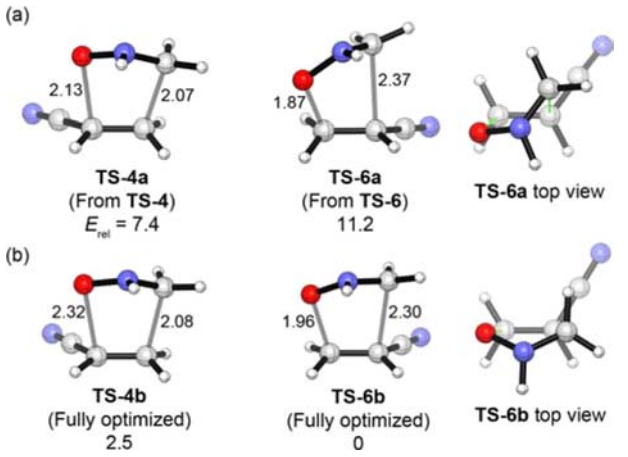

Figure 3. (a) Truncated analogues of **TS-4** and **TS-6**, representing the five-membered bond-forming array. **TS-4a** and **TS-6a** were obtained by replacing the alkyl groups of **TS-4** and **TS-6** by hydrogen atoms at a fixed distance of 1.09 Å. (b) The corresponding fully optimized transition states for cycloadditions of methylene nitrone with acrylonitrile. Potential energies (all relative to **TS-6b**; ZPE-exclusive) are given in kcal/mol [M06-2X/6-311+G(d,p)].

arrays from **TS-4** and **TS-6** after replacement of the alkyl groups by hydrogen atoms (**TS-4a** and **TS-6a**).[17] Fully optimized versions of these transition structures are also shown (**TS-4b** and **TS-6b**). While the fully optimized transition states show a regioselectivity of 2.5 kcal/mol ($\Delta\Delta E^{\ddagger}$) in favor of **6**, the distorted arrays from the intramolecular TSs favor **4** by 3.8 kcal/mol. The intrinsic selectivity is reversed in the intramolecular structures because the alkene fragment is more distorted and is oriented less ideally for bonding to the nitrone. This is most clearly seen in the top views of the transition states included in Figure 3.

We also investigated the possible influence of the different solvents used for the intramolecular 1,3-dipolar cycloaddition under kinetic and thermodynamic conditions. CPCM calculations on **TS-4**−**TS-6** in methanol and chlorobenzene gave the solution-phase activation energies shown in Figure 2. Solvation raises the barriers fairly uniformly by 1−2 kcal/mol and mirrors the gas-phase prediction that **4** is the kinetic product. Likewise, **6** remains the predicted thermodynamic product in solution (see the Supporting Information).

These calculations offer insight into the mechanism responsible for the formation of transient **5** during the thermal isomerization of **4** to **6** (Scheme 1). At 180 °C in chlorobenzene, the activation energies for the formation of **4**−**6** from the common nitrone **3** correspond to a 80:3:17 kinetic selectivity (**4**:**5**:**6**). The small proportion of **5** in this ratio is not sufficient to explain the quantities of **5** detected experimentally. The alternative route suggested previously,[2d] involving bicyclic species **8** (Scheme 2), is likely more significant.

Racemization. Calculations were also performed to explore mechanisms for the racemization of (+)-**6** at high temperatures. We searched for various types of transition states that could lead to the formation of bicyclic intermediate **8** from **5** or **4** (Scheme 2). The proposed[2d] interconversion **5** → **8** → **4** is related to the Cope elimination reactions of *N*-ethyl hydroxylamines,[18−20] but with the added requirement of one or more protonation/deprotonation steps. Attempts to locate unimolecular (protonated) transition states related to those of known Cope elimination reactions[21] gave only high-energy structures ($\Delta G^{\ddagger} \geq$ 58 kcal/mol; see the Supporting Information), while a transition state for the C−N bond-formation step of an intramolecular conjugate addition of **8**[20c] could not be located. The conversion **5** → **8** → **4** most likely involves ionic intermediates and proton-transfer steps mediated by adventitious hydroxylic molecules. Because of the ionic character of the intermediates and the likely stabilization of the intermediates and transition states by adventitious hydroxylic molecules, it is difficult to compare the rates of these elimination reactions with those of the neutral, unimolecular (retro-)1,3-dipolar cycloadditions. Upon optimization in a solvent continuum,[22] we were able to locate the zwitterionic intermediate **5-zw**, derived from **5**. Its free energy in chlorobenzene (24.4 kcal/mol) was 1.6 kcal/mol lower than that of **TS-5** (26.0 kcal/mol; Figure 2). We assume that the elimination reactions **5** → **8** and **4** → **8** are facile in solution.

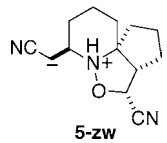

5-zw

We also explored an alternative racemization pathway in which the piperidine ring opens directly from (+)-**6**. This new pathway is shown in Scheme 3, together with the original proposal.[2d] Opening of the piperidine ring of (+)-**6** affords bicyclic species **9**. Subsequent recyclization from the opposite face gives intermediate **10′**, which is also the species that would result from a 6,6,5 cycloaddition onto the more crowded face of the nitrone. Retro-1,3-dipolar cycloaddition of **10′** followed by recycloaddition from the less hindered face furnishes (−)-**6**. A second alternative pathway involves these species in a different sequence: (+)-**6** → **3** → **10** → **9′** → (−)-**6**.

dx.doi.org/10.1021/ja300002k | *J. Am. Chem. Soc.* 2012, 134, 12010−12015

Scheme 3. Revised Mechanism for the Interconversion of 6,6,5- and 6,5,5-Tricyclic Species[a]

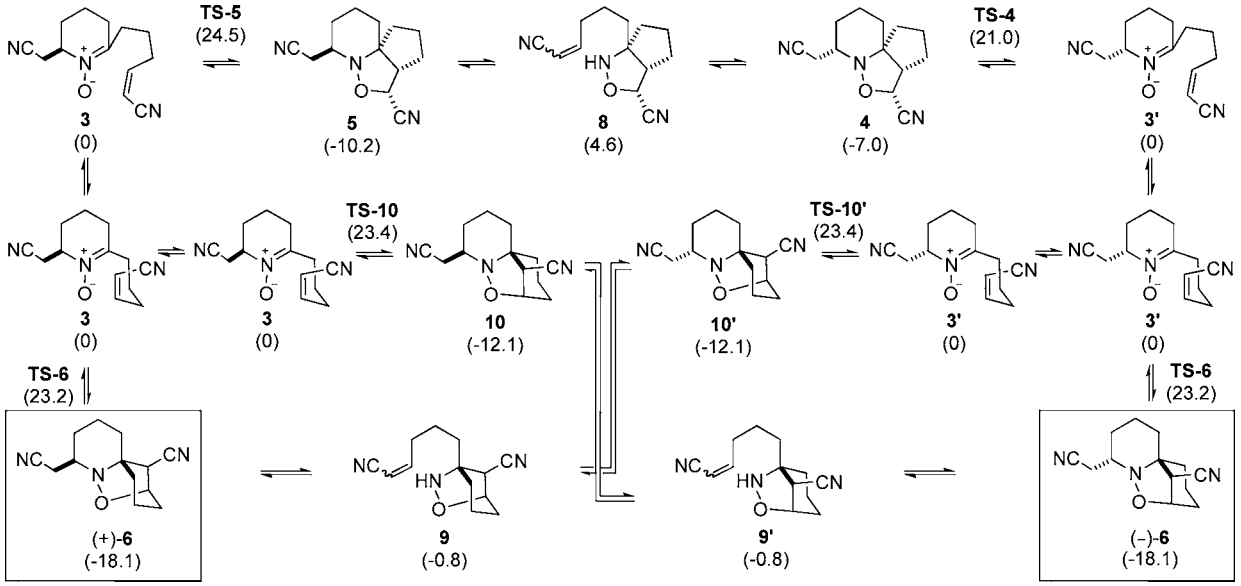

[a]M06-2X Gibbs free energies relative to nitrone **3** are shown (gas-phase, kcal/mol). The different arrangements drawn for the $(CH_2)_3CN$ chain in **3** and **3′** are shown only to indicate the type of tricyclic framework that is to be formed upon cycloaddition; the energy listed underneath each of these structures is the energy of the most stable conformer.

The energies of the transition states and intermediates in the two racemization pathways are included in Scheme 3. Data for species **9**, **10**, and **TS-10** are included in the Supporting Information. The piperidine ring-opening steps are assumed not to be rate-limiting. The racemization pathway starting from (+)-**6** and involving **9**/**10′**/**3′** has a barrier of 23.4 kcal/mol (as does an alternative pathway involving **3**/**10**/**9′**), while the less direct route involving **3**/**5**/**8**/**4**/**3′** has a barrier of 24.5 kcal/mol. These barriers correspond to a ratio of 3:3:1 at 185 °C; hence, each of the three pathways is expected to be mechanistically significant. The tricyclic species **10** has not yet been detected, but trapping experiments are currently underway.

We also considered the possibility that nitrone **3** can revert to the oxime **2** at elevated temperatures (Figure 4). This would provide an alternative route for the interconversion of (+)-**6** and (−)-**6** but would also be expected to lead to some *Z*/*E* alkene scrambling. Grigg[4] has shown that additions of oximes to electron-deficient alkenes (1,3-azaprotio cyclotransfer reactions) are concerted processes. Figure 4 shows concerted transition states for ring opening of nitrone **3** to give an oxime with either a *Z* or an *E* pendant alkene. There is a small *Z*/*E* selectivity (1.3 kcal/mol). The computed barriers indicate that ring opening to give a *Z* alkene is of minor importance at 185 °C.

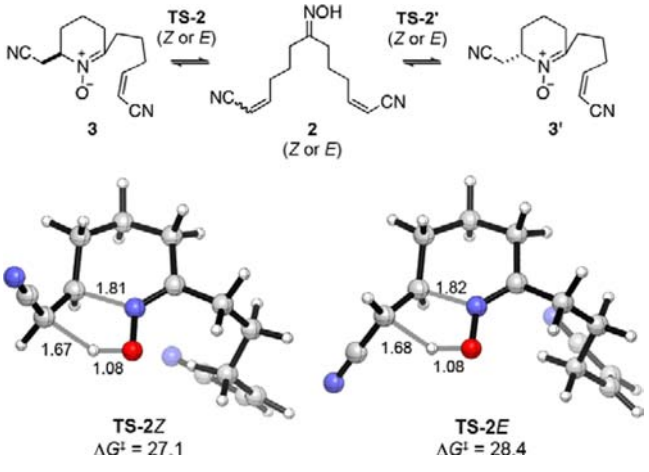

Figure 4. Transition states for ring opening of nitrone **3** to give an oxime with a *Z* or *E* pendant alkene (reverse 1,3-azaprotio cyclotransfer reactions). The M06-2X activation energies are shown (gas phase, kcal/mol). Bond lengths are in Å.

CONCLUSION

Density functional theory calculations have identified the factors responsible for kinetic and thermodynamic control in the intramolecular 1,3-dipolar cycloadditions of the *C*-(cyanoalkenyl)nitrone employed in the Holmes−Stockman synthesis of histrionicotoxin. M06-2X and B3LYP calculations correctly predict that the 6,6,5-tricyclic species **6** is the thermodynamic product of the cycloaddition and that the 6,5,5-tricyclic species **4** is the kinetic product. The transition state leading to **6** is higher in energy due to the poor overlap between the nitrone and the alkene that is enforced by the tether. The observed racemization of (+)-**6** is suggested to occur by three pathways − two commencing with retro-1,3-dipolar cycloaddition and the other commencing with an elimination reaction that opens the piperidine ring. These pathways operate in parallel at elevated temperatures. A comprehensive understanding of the mechanistic pathway leading to tricyclic bisnitrile **6** provides an opportunity to address the synthesis of biologically important analogues that hitherto have not been accessible as well as to consider enantioselective syntheses from a simple achiral precursor.

dx.doi.org/10.1021/ja300002k | J. Am. Chem. Soc. 2012, 134, 12010−12015

■ ASSOCIATED CONTENT

Supporting Information

Calculated geometries and energies and complete refs 7 and 11. This material is available free of charge via the Internet at http://pubs.acs.org.

■ AUTHOR INFORMATION

Corresponding Author

ekrenske@unimelb.edu.au; houk@chem.ucla.edu; aholmes@unimelb.edu.au

Notes

The authors declare no competing financial interest.

■ ACKNOWLEDGMENTS

We thank NIH (FIRCA Project 5R03TW007177-02 to V.A. and S.A.), NSF (CHE-0548209 to K.N.H.), the Australian Research Council (DP0985623 to E.H.K.), the ARC Centre of Excellence for Free Radical Chemistry and Biotechnology (funding to E.H.K.), and CSIRO (fellowship to A.B.H.) for generous financial support. Computing resources used in this work were provided by the National Center for High Performance Computing of Turkey UYBHM (Grants 20452008 and 11062010), UCLA Academic Technology Services/Institute for Digital Research and Education, the National Computational Infrastructure National Facility (Australia), and the University of Melbourne School of Chemistry.

■ REFERENCES

(1) (a) Oppolzer, W.; Siles, S.; Snowden, R. L.; Bakker, B. H.; Petrzilka, M. *Tetrahedron* **1985**, *41*, 3497−3509. (b) LeBel, N. A.; Balasubramanian, N. *J. Am. Chem. Soc.* **1989**, *111*, 3363−3368. (c) Fox, M. E.; Holmes, A. B.; Forbes, I. T.; Thompson, M. *J. Chem. Soc., Perkin Trans. 1* **1994**, 3379−3395. (d) Davison, E. C.; Holmes, A. B.; Forbes, I. T. *Tetrahedron Lett.* **1995**, *36*, 9047−9050. (e) Davison, E. C.; Forbes, I. T.; Holmes, A. B.; Warner, J. A. *Tetrahedron* **1996**, *52*, 11601−11624. (f) Holmes, A. B.; Bourdin, B.; Collins, I.; Davison, E. C.; Rudge, A. J.; Stork, T. C.; Warner, J. A. *Pure Appl. Chem.* **1997**, *69*, 531−536. (g) Martin, J. N.; Jones, R. C. F. In *Synthetic Applications of 1,3-Dipolar Cycloaddition Chemistry Toward Heterocycles and Natural Products*; Padwa, A., Pearson, W. H., Eds.; Wiley: Hoboken, NJ, 2003; pp 1−81.

(2) (a) Williams, G. M.; Roughley, S. D.; Davies, J. E.; Holmes, A. B.; Adams, J. P. *J. Am. Chem. Soc.* **1999**, *121*, 4900−4901. (b) Smith, C. J.; Holmes, A. B.; Press, N. J. *Chem. Commun.* **2002**, 1214−1215. (c) Davison, E. C.; Fox, M. E.; Holmes, A. B.; Roughley, S. D.; Smith, C. J.; Williams, G. M.; Davies, J. E.; Raithby, P. R.; Adams, J. P.; Forbes, I. T.; Press, N. J.; Thompson, M. J. *J. Chem. Soc., Perkin Trans. 1* **2002**, 1494−1514. (d) Horsley, H. T.; Holmes, A. B.; Davies, J. E.; Goodman, J. M.; Silva, M. A.; Pascu, S. I.; Collins, I. *Org. Biomol. Chem.* **2004**, *2*, 1258−1265. (e) Brasholz, M.; Macdonald, J. M.; Saubern, S.; Ryan, J. H.; Holmes, A. B. *Chem.—Eur. J.* **2010**, *16*, 11471−11480. (f) Brasholz, M.; Johnson, B. A.; Macdonald, J. M.; Polyzos, A.; Tsanaktsidis, J.; Saubern, S.; Holmes, A. B.; Ryan, J. H. *Tetrahedron* **2010**, *66*, 6445−6449.

(3) (a) Stockman, R. A. *Tetrahedron Lett.* **2000**, *41*, 9163−9165. (b) Stockman, R. A.; Sinclair, A.; Arini, L. G.; Szeto, P.; Hughes, D. L. *J. Org. Chem.* **2004**, *69*, 1598−1602.

(4) (a) Grigg, R.; Markandu, J.; Perrior, T.; Surendrakumar, S.; Warnock, W. J. *Tetrahedron* **1992**, *48*, 6929−6952. (b) Grigg, R.; Markandu, J.; Surendrakumar, S.; Thornton-Pett, M.; Warnock, W. J. *Tetrahedron* **1992**, *48*, 10399−10422. (c) Grigg, R.; Perrior, T. R.; Sexton, G. J.; Surendrakumar, S.; Suzuki, T. *J. Chem. Soc., Chem. Commun.* **1993**, 372−374. (d) Dondas, H. A.; Grigg, R.; Hadjisoteriou, M.; Markandu, J.; Thomas, W. A.; Kennewell, P. *Tetrahedron* **2000**, *56*, 10087−10096. (e) Dondas, H. A.; Grigg, R.; Hadjisoteriou, M.; Markandu, J.; Kennewell, P.; Thornton-Pett, M. *Tetrahedron* **2001**, *57*, 1119−1128. (f) Dondas, H. A.; Fishwick, C. W. G.; Grigg, R.; Thornton-Pett, M. *Tetrahedron* **2003**, *59*, 9997−10007.

(5) We recently reported a flow synthesis of the histrionicotoxin precursor **6** (ref 2f). A mixture of ketone **1** and $NH_2OH{\cdot}HCl$/NaOAc in methanol was subjected to a two-stage heating process (50 °C then 150 °C), leading to a 48% yield of **6** after purification.

(6) (a) Lee, C.; Yang, W.; Parr, R. G. *Phys. Rev. B* **1988**, *37*, 785−789. (b) Becke, A. D. *J. Chem. Phys.* **1993**, *98*, 1372−1377. (c) Becke, A. D. *J. Chem. Phys.* **1993**, *98*, 5648−5652.

(7) Frisch, M. J.; et al. *Gaussian 03*, revision E.01; Gaussian, Inc.: Wallingford, CT, 2004.

(8) *Spartan'08*; Wavefunction, Inc.: Irvine, CA.

(9) (a) Gonzalez, C.; Schlegel, H. B. *J. Chem. Phys.* **1989**, *90*, 2154−2161. (b) Gonzalez, C.; Schlegel, H. B. *J. Phys. Chem.* **1990**, *94*, 5523−5527.

(10) (a) Zhao, Y.; Truhlar, D. G. *Theor. Chem. Acc.* **2008**, *120*, 215−241. (b) Zhao, Y.; Truhlar, D. G. *Acc. Chem. Res.* **2008**, *41*, 157−167.

(11) Frisch, M. J.; et al. *Gaussian 09*, revision A.02; Gaussian, Inc.: Wallingford, CT, 2009.

(12) (a) Barone, V.; Cossi, M. *J. Phys. Chem. A* **1998**, *102*, 1995−2001. (b) Cossi, M.; Rega, N.; Scalmani, G.; Barone, V. *J. Comput. Chem.* **2003**, *24*, 669−681.

(13) Legault, C. Y. *CYLview*, version 1.0b; Université de Sherbrooke: Sherbrooke, QC, 2009; http://www.cylview.org.

(14) (a) Ess, D. H.; Houk, K. N. *J. Phys. Chem. A* **2005**, *109*, 9542−9553. (b) Lan, Y.; Zou, L.; Cao, Y.; Houk, K. N. *J. Phys. Chem. A* **2011**, *115*, 13906−13920.

(15) Jones, G. O.; Guner, V. A.; Houk, K. N. *J. Phys. Chem. A* **2006**, *110*, 1216−1224.

(16) (a) Krenske, E. H.; Houk, K. N.; Holmes, A. B.; Thompson, J. *Tetrahedron Lett.* **2011**, *52*, 2181−2184. (b) Krenske, E. H.; Davison, E. C.; Forbes, I. T.; Warner, J. A.; Smith, A. L.; Holmes, A. B.; Houk, K. N. *J. Am. Chem. Soc.* **2012**, *134*, 2434−2441.

(17) Hydrogen atoms were appended at a fixed distance of 1.09 Å.

(18) (a) Cram, D. J.; McCarty, J. E. *J. Am. Chem. Soc.* **1954**, *76*, 5740−5745. (b) Bach, R. D.; Andrzejewski, D.; Dusold, L. R. *J. Org. Chem.* **1973**, *38*, 1742−1743. (c) Chiao, W.-B.; Saunders, W. H., Jr. *J. Am. Chem. Soc.* **1978**, *100*, 2802−2805. (d) Kwart, H.; George, T. J.; Louw, R.; Ultee, W. *J. Am. Chem. Soc.* **1978**, *100*, 3927−3928.

(19) (a) Komaromi, I.; Tronchet, J. M. J. *J. Phys. Chem. A* **1997**, *101*, 3554−3560. (b) Acevedo, O.; Jorgensen, W. L. *J. Am. Chem. Soc.* **2006**, *128*, 6141−6146. (c) Beauchemin, A. M.; Moran, J.; Lebrun, M.-E.; Séguin, C.; Dimitrijevic, E.; Zhang, L.; Gorelsky, S. I. *Angew. Chem., Int. Ed.* **2008**, *47*, 1410−1413. (d) Moran, J.; Gorelsky, S. I.; Dimitrijevic, E.; Lebrun, M.-E.; Bédard, A.-C.; Séguin, C.; Beauchemin, A. M. *J. Am. Chem. Soc.* **2008**, *130*, 17893−17906. (e) Bourgeois, J.; Dion, I.; Cebrowski, P. H.; Loiseau, F.; Bédard, A.-C.; Beauchemin, A. M. *J. Am. Chem. Soc.* **2009**, *131*, 874−875.

(20) (a) Ciganek, E. *J. Org. Chem.* **1990**, *55*, 3007−3009. (b) Oppolzer, W.; Spivey, A. C.; Bochet, C. G. *J. Am. Chem. Soc.* **1994**, *116*, 3139−3140. (c) Ciganek, E.; Read, J. M., Jr.; Calabrese, J. C. *J. Org. Chem.* **1995**, *60*, 5795−5802.

(21) (a) Niu, D.; Zhao, K. *J. Am. Chem. Soc.* **1999**, *121*, 2456−2459. (b) O'Neil, I. A.; Cleator, E.; Southern, J. M.; Bickley, J. F.; Tapolczay, D. J. *Tetrahedron Lett.* **2001**, *42*, 8251−8254. (c) Moglioni, A. G.; Muray, E.; Castillo, J. A.; Álvarez-Larena, Á.; Moltrasio, G. Y.; Branchadell, V.; Ortuño, R. M. *J. Org. Chem.* **2002**, *67*, 2402−2410.

(22) The geometry of **5-zw** was optimized in methanol. Attempted optimization in chlorobenzene led to C−N bond cleavage.